

# Development of a Continuous-Flow System for Asymmetric Hydrogenation Using Self-Supported Chiral Catalysts

Lei Shi, Xingwang Wang, Christian A. Sandoval, Zheng Wang, Hongji Li, Jiang Wu, Liting Yu, and Kuiling Ding\*<sup>[a]</sup>

*Dedicated to Professor Youcheng Liu on the occasion of his 90th birthday*

**Abstract:** Well-designed, self-assembled, metal–organic frameworks were constructed by simple mixing of multi-topic MonoPhos-based ligands (**3**; MonoPhos=chiral, monodentate phosphoramidites based on the 1,1'-bi-2-naphthol platform) and [Rh(cod)<sub>2</sub>]BF<sub>4</sub> (cod=cycloocta-1,5-diene). This self-supporting strategy allowed for simple and efficient catalyst immobilization without the use of extra added support, giving well-characterized, insoluble (in toluene) polymeric materials (**4**). The resulting self-supported catalysts (**4**) showed outstanding catalytic performance for the asymmetric hydrogenation of a number of  $\alpha$ -dehydroamino acids (**5**) and 2-aryl enamides (**7**) with enantiomeric excess (*ee*) ranges of 94–

98% and 90–98%, respectively. The linker moiety in **4** influenced the reactivity significantly, albeit with slight impact on the enantioselectivity. Acquisition of reaction profiles under steady-state conditions showed **4h** and **4i** to have the highest reactivity (turnover frequency (TOF)=95 and 97 h<sup>-1</sup> at 2 atm, respectively), whereas appropriate substrate/catalyst matching was needed for optimum chiral induction. The former was recycled 10 times without loss in *ee* (95–96%), although a

drop in TOF of approximately 20% per cycle was observed. The estimation of effective catalytic sites in self-supported catalyst **4e** was also carried out by isolation and hydrogenation of catalyst–substrate complex, showing about 37% of the Rh<sup>I</sup> centers in the self-supported catalyst **4e** are accessible to substrate **5c** in the catalysis. A continuous flow reaction system using an activated C/**4h** mixture as stationary-phase catalyst for the asymmetric hydrogenation of **5b** was developed and run continuously for a total of 144 h with >99% conversion and 96–97% enantioselectivity. The total Rh leaching in the product solution is 1.7% of that in original catalyst **4h**.

**Keywords:** asymmetric catalysis • continuous flow system • heterogeneous catalysis • hydrogenation • self-supported catalysts

## Introduction

The use of homogeneous asymmetric hydrogenation catalysts to provide enantiomerically enriched products is of central importance in modern synthetic chemistry and a core technology in the pharmaceutical, agrochemical, and fine chemical industries.<sup>[1]</sup> Although such homogeneous sys-

tems offer the advantages of high enantioselectivity and catalytic activity under mild reaction conditions, the difficulties associated with recovery and reuse of expensive (toxic) chiral catalysts, and catalyst–product separation have hampered their more widespread application. A promising solution to such limitations is the immobilization and subsequent recycling of the chiral catalysts employed.<sup>[2]</sup> Due to the significant importance of asymmetric hydrogenation (AH), this endeavor has attracted a great deal of interest from both academic and industrial societies in recent years.<sup>[2,3]</sup>

Presently, the most common and successful strategy for heterogeneous asymmetric catalysis has been the immobilization of well-developed and understood homogeneous catalysts. Several major heterogenization approaches have been utilized:<sup>[2,4]</sup> covalent attachment to inorganic and organic (soluble and insoluble) polymers, dendrimers, and

[a] L. Shi, Dr. X. Wang, Prof. Dr. C. A. Sandoval, Prof. Dr. Z. Wang, H. Li, J. Wu, L. Yu, Prof. Dr. K. Ding  
State Key Laboratory of Organometallic Chemistry  
Shanghai Institute of Organic Chemistry  
Chinese Academy of Sciences  
345 Lingling Road, Shanghai 200032 (P.R. China)  
Fax: (+86) 21-6416-6128  
E-mail: kding@mail.sioc.ac.cn

Supporting information for this article is available on the WWW under <http://dx.doi.org/10.1002/chem.200900899>.

membrane supports; noncovalent catalyst adhesion (ion exchange, electrostatic attraction); encapsulation of catalyst; and use of biphasic systems (aqueous/organic solvent, ionic liquid). Such immobilization strategies have inherent advantages and disadvantages, although no method has thus far proven to be general. Moreover, despite some noteworthy exceptions in which the immobilized system outperforms the homogeneous counterparts,<sup>[5]</sup> support-anchored heterogeneous catalysts have generally displayed reduced activity and/or enantioselectivity. This can mostly be attributable to disruption of the optimum metal–ligand relationship crucial for catalysis (geometric and chemical) and/or undesired interactions between the metal–ligand unit and the support employed.

A recently reported promising immobilization strategy for heterogeneous asymmetric catalysis is the “self-supporting” approach<sup>[6]</sup> inspired by recent development of coordination polymer chemistry<sup>[7]</sup> and its application in catalysis.<sup>[7b,e,8,9]</sup> In the self-supporting strategy for chiral catalyst immobilization, heterogenization of the catalysts is achieved by the self-assembly of chiral multitopic ligands and reactive metal ions to give homochiral metal–organic coordination polymers or networks (Figure 1). The high dimensionality of obtained microstructures in the coordination polymers may result in extremely low solubility in common organic solvents, rendering the system heterogeneous in nature and thus providing an excellent opportunity for heterogeneous asymmetric catalysis. Furthermore, such structures can replicate the key features of a homogeneous molecular catalyst

and thus exhibit a somewhat predictable catalytic behavior, since the stereochemical properties of the chiral ligands and corresponding catalysts are expected to remain intact by virtue of the mild synthesis employed. The isolation of the reactive sites to prevent the interaction of catalytically active centers can be readily achieved by tuning the structure of the spacer in the multitopic ligand. Since the first report on the use of self-assembled microporous homochiral organic–metal material for enantioselective catalysis (with 8% enantioselectivity for a kinetic resolution of racemic 1-phenyl-2-propanol) in 2000,<sup>[10]</sup> several types of homogeneous chiral catalysts have been effectively immobilized based on this strategy without the use of any extra supports. The resulting homochiral assemblies have met with notable success in the heterogeneous catalysis of asymmetric catalytic carbonyl-ene reaction,<sup>[11]</sup> Michael addition,<sup>[11a]</sup> alkylation,<sup>[12]</sup> olefin epoxidation,<sup>[13]</sup> sulfoxidation,<sup>[11c]</sup> cyclopropanation,<sup>[14]</sup> ring-opening of epoxide,<sup>[15]</sup> and hydrogenation.<sup>[16]</sup> These self-supported chiral catalysts can usually be recycled for several consecutive runs, and in some cases the product enantioselectivities were comparable to or even better than the homogeneous counterparts (up to 99.9%).

Previously in a communication<sup>[16c]</sup> we have reported the preliminary results on the development of the self-supporting strategy for immobilization of Feringa and co-workers’ MonoPhos (**1**, Scheme 1)/Rh<sup>I</sup> catalyst<sup>[17a]</sup> in asymmetric hydrogenation of  $\alpha$ -dehydroamino acids and enamides.<sup>[17]</sup> The approach was inspired by the generally accepted understanding that the catalytically active species involved in the reactions should contain two monodentate phosphorous ligands coordinatively bonded to one Rh<sup>I</sup> cation.<sup>[18]</sup> Thus, through assembly of a polytopic monodentate phosphorus ligand with an appropriate Rh<sup>I</sup> precursor, a catalytically active P–Rh–P motif could be incorporated into the backbone of the resulting coordination polymer. The thus immobilized MonoPhos/Rh catalysts showed good reactivity (> 99% conversion) and excellent enantioselectivities (94–97% *ee*) in the asymmetric hydrogenation of  $\alpha$ -dehydroamino acid and amide derivatives. For the catalyst reuse test, the conversion remained quantitative during seven runs under the experimental conditions (1 mol% cat., 40 atm of H<sub>2</sub>, 10 h); however, a gradual loss of enantioselectivity was observed with recycling (95–89% *ee*). To overcome such a problem commonly seen in a heterogenized catalyst, it is necessary to carry out a comprehensive study for understanding the inherent properties of the immobilized catalysts, including the structure–catalytic performance correlation of these metal–organic coordination polymers.

Herein we describe the details on the synthesis, characterization, and catalytic performance of a series of self-supported catalysts built up from variably linked multitopic MonoPhos ligands and a Rh<sup>I</sup> metal salt. The efficient heterogeneous asymmetric hydrogenation of  $\alpha$ -dehydroamino acids and enamides catalyzed by the resultant assemblies are detailed. Presentation and discussion of comprehensive studies of the inherent properties and recyclable nature of such metal–organic polymers, and differences in their catalytic perfor-

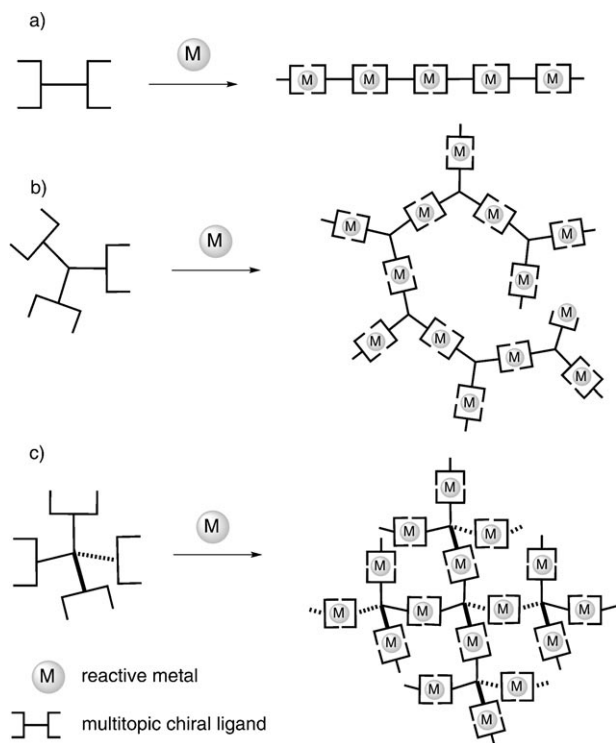
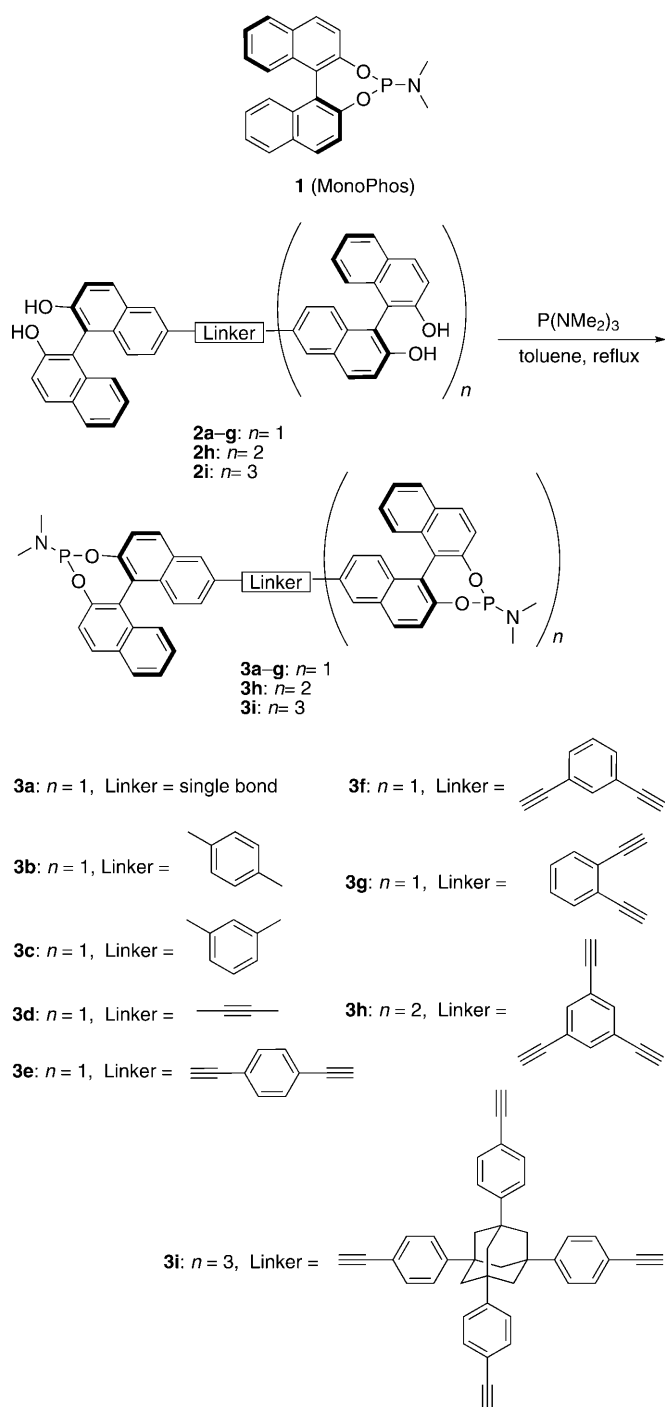


Figure 1. Schematic representation of self-supported heterogeneous catalysts from the reaction of metal ions with a) ditopic, b) tritopic (planar), and c) tetratopic (tetrahedral) chiral ligands.

## Results and Discussion



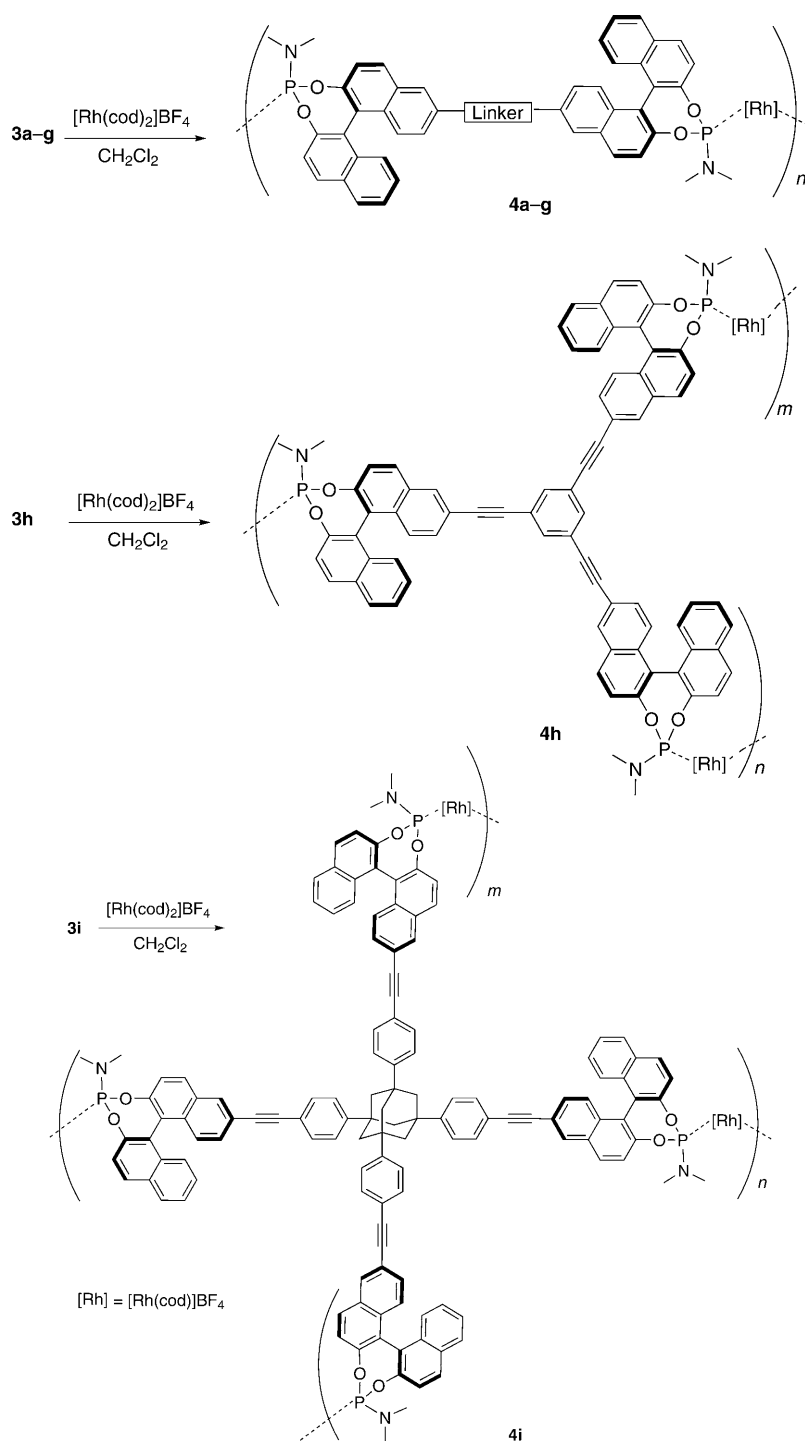
Scheme 1. Synthesis of MonoPhos (**1**)-based multitopic phosphoramidite ligands **3a-i**. In the case of ligand **3i**, (*R*)-BINOL was used as the starting material.

mance are provided. Furthermore, the development and performance of a three-phase (gas-liquid-solid) continuous flow reactor for asymmetric hydrogenation is described, which has provided a useful approach for stabilizing the self-supported catalyst.

For a self-supported chiral catalyst constructed on the conceptual base shown in Figure 1, the stereochemical characteristics of the multitopic ligand should exhibit some impact on the microstructure of the resulting assembly, and thus may exert significant influence on its catalytic performance in a given reaction. Such an effect of the bridging spacer in the multitopic ligand, for example, has been observed in the heterogenization of Shibasaki's BINOL/La (BINOL = 1,1'-bi-2-naphthol) catalyst for enantioselective epoxidation of  $\alpha,\beta$ -unsaturated ketones.<sup>[13a]</sup> In the present work, four types of multitopic MonoPhos ligands (**3a-3i**; Scheme 1) with different bridging linkers, including linear (**3a-b**, **3d,e**), bent (**3c**, **3f,g**), trigonal-planar (**3h**), and tetrahedral (**3i**) spacers, were synthesized to investigate the potential impact of the spatial arrangement of chiral units ((*S*)-MonoPhos) in the ligands on the catalytic properties of the self-supported MonoPhos/Rh catalysts in asymmetric hydrogenation. According to the principle shown in Figure 1 for generation of self-supported heterogeneous catalysts, these structurally diverse ligands are expected to result in a variety of heterogeneous chiral catalysts with different spatial arrangement when they react with a  $\text{Rh}^{\text{I}}$  cation.

**Multitopic ligand synthesis:** Ligand **2a** was prepared by Suzuki coupling of (*S*)-6-bromo-2,2'-di(methoxymethoxy)-1,1'-binaphthyl with (*S*)-6-(MeO)<sub>2</sub>B-2,2'-di(methoxymethoxy)-1,1'-binaphthyl, followed by acidic deprotection of methoxymethyl groups.<sup>[11b]</sup> In similar fashion, ligands **2b,c** were obtained by the reaction of *para*- and *meta*-phenylene-diboronic acid with (*S*)-6-bromo-2,2'-di(methoxymethoxy)-1,1'-binaphthyl, followed by acidic deprotection of methoxymethyl groups. The syntheses of other ligands (**2d-i**) were achieved by the Pd-catalyzed Sonogashira reactions of methoxymethyl (MOM)-protected, 6-ethynyl-substituted BINOL derivatives with the corresponding aryl bromides or a MOM-protected, 6-bromo-substituted BINOL derivative with the corresponding aryl acetylene, followed by deprotection of the MOM groups of the Sonogashira coupling products by acidic hydrolysis.<sup>[13a]</sup> The linker-bridged poly-MonoPhos ligands **3a-i** were prepared by the reaction of hexamethylphosphoramide (HMPT) with corresponding multitopic BINOL ligands **2a-i** in good yields (64–85%, Scheme 1).<sup>[16c]</sup> All multitopic ligands have been characterized by standard <sup>1</sup>H and <sup>31</sup>P NMR spectroscopy, optical rotation, FTIR, mass spectroscopy (MS), and high-resolution mass spectroscopic (HRMS) analysis. They are soluble in common organic solvents, air stable, and may be stored indefinitely under argon.

**Catalyst synthesis and characterization:** The self-supported catalysts **4a-i** were synthesized by assembly of Rh metal ions with the MonoPhos-based multitopic ligands **3a-i**, as outlined in Scheme 2. The multitopic phosphoramidite ligand **3** and catalyst precursor  $[\text{Rh}(\text{cod})_2]\text{BF}_4$  (cod = cycloocta-1,5-diene) were dissolved in dichloromethane. The ad-



Scheme 2. Synthesis of self-supported catalysts **4a–i**.

dition of a solution of **3** to that of  $[\text{Rh}(\text{cod})_2]\text{BF}_4$  afforded a suspension or a precipitate immediately. After stirring for 30 min, the solvent was removed to give the orange self-supported catalyst **4** in almost quantitative yields. The orange solids **4a–g** were sparingly soluble in  $\text{CH}_2\text{Cl}_2$ , whereas **4h** and **4i** were insoluble in the same solvent. All self-supported catalysts (**4a–i**) were completely insoluble in toluene, fulfilling the basic prerequisites of heterogeneous catalysis. Ac-

cordingly, toluene was selected as the reaction medium for the heterogeneous hydrogenation of olefin derivatives.

Elemental analysis results showed that the composition of the resulting solids (**4a–i**) were consistent with their corresponding expected structures. In each case, the ratio of the MonoPhos unit(s) to that of Rh centers was calculated to be closely equal to two. The salient features of the self-supporting strategy include the high overall ligand content and well-isolated coordinating units by linking spacers, and accordingly high density of active sites in the resulting materials. This should be easily understandable since no extra carrier (mass) was introduced during the catalyst generation. Assuming a perfect alternating copolymerization of the metal with the ligand has occurred during polymer formation, the maximum density of the catalytically active Rh units was expected to range from  $0.39$  to  $0.98 \text{ mmol g}^{-1}$  (mmol of Rh per gram of the polymer) for **4a–i**.<sup>[19]</sup> Such an assumption is reasonable considering that metal–ligand coordination (binding) is essential for polymer formation and that such a structural motif persists during and after hydrogenation itself, that is, no hydrogenation is observed with filtrate alone after catalyst filtration following hydrogenation (discussed below).

A comparison of the chemical shifts in the solid-state  $^{31}\text{P}$  cross-polarization magic-angle-spinning (CP-MAS) NMR spectra of multitopic ligand

**3h,i** and their assembled polymers **4h,i** (see the Supporting Information) with those of **1** and its  $\text{Rh}^{\text{I}}$  complex clearly demonstrated a similar coordination pattern in the solid state.  $^{31}\text{P}$  CP-MAS NMR spectroscopy of **1** shows a broad peak centered at  $\delta = 148.6$  ppm, which moves upfield to  $\delta = 135.3$  ppm upon formation of the  $\text{Rh–I}_2$  complex (see Figure S3 in the Supporting Information). Similarly, resonances for **3h** and **3i** shift from  $\delta = 148.8$  ppm to  $\delta = 137.3$  and



employed for the catalysis of the hydrogenation of **5b** under the same experimental conditions. No product was observed. Furthermore, inductively coupled plasma (ICP) atomic emission spectroscopy (AES) analyses indicated no detectable rhodium (detection limit of ICP-AES for Rh is 1 ppm) had leached into the organic solution (<0.85% of the supported rhodium in **4d**). Thus, the present systems are unambiguously heterogeneous without metal and/or ligand leaching into the liquid phase.

As can be envisioned from Figure 1, when using the self-supporting strategy for heterogenization of homogeneous chiral catalysts, the stereochemical characteristics of the multitopic ligands should in principle have a substantial influence on the microstructures of the resulting homochiral metal-organic polymers. This, in turn, is expected to exert an impact on the enantioselectivity and activity of the catalysis. In fact, catalysts **4** prepared in the same way, with the only difference lying in their spacer moieties, displayed different catalytic performance for the asymmetric hydrogenation of  $\alpha$ -dehydroamino acid methyl esters (**5**) under the standard conditions ( $[4]=2$  mM,  $[5]=0.2$  M,  $P(H_2)=40$  atm,  $T=25^\circ\text{C}$ ,  $t=10$  h, toluene solvent) shown in Table 1. The obtained *ee* values for products **6** were comparable to the homogeneous Rh-**1**<sub>2</sub> catalyst, consistently giving values between 94 and 98%. Interestingly, the *ee* values were found to be subtly influenced by the linker used in the multitopic ligand and the particular substrate structure. Thus, although the highest enantioselectivity for **6a** and **6b** was obtained with the catalyst **4i** generated from tetratopic **3i** (97 and 98%, respectively), ditopic-ligand-based catalyst **4f** yielded the highest *ee* value for **6c** (97%).

Under the same conditions, asymmetric hydrogenations of 2-aryl-substituted enamides (**7**) were similarly conducted, and the results are summarized in Table 2. For the simple phenyl derivative **7a** the highest chiral induction (98% *ee*) was obtained with **4f** catalyst, whereas some other ditopic-ligand-based catalysts (**4a**, **4d**, and **4e**) similarly gave high enantioselectivity (97%). In contrast, tetratopic-ligand-based catalyst **4i** promotes the hydrogenation of **7a** in only 93% *ee*. In general, the performance of self-supported catalysts was comparable to the homogeneous MonoPhos-based (Rh-**1**<sub>2</sub>) system that yields **8a** in 95% *ee* under the same conditions. Overall, the observed enantioselectivities for a number of aryl enamides were found to also be dependent on catalyst-linker/substrate-structure matching. For example, catalyst **4a** gave **8c** in 96% *ee*, whereas **4c** gave the same product in 90% *ee*. The catalysis was not obviously influenced by electron-donating or -withdrawing groups on the aryl substituent in **7**. Interestingly, the observed differences in enantioselectivity are only marginal for a number of ligand types, while noting that all catalysts provide respectable chiral induction. This suggests that the actual environment about the metal-coordinating moiety (P ligand) is not detrimentally affected by the self-supporting process itself. This is in contrast to some other immobilization techniques employed in which a consequent large drop in enantioselectivity may occur.<sup>[4]</sup> This constitutes an attractive feature of

Table 2. Asymmetric hydrogenation of 2-aryl-substituted enamides (**7**) catalyzed by self-assembled catalyst (**4**).<sup>[a]</sup>

**7a:** R = C<sub>6</sub>H<sub>5</sub>  
**7b:** R = 4-CH<sub>3</sub>C<sub>6</sub>H<sub>4</sub>  
**7c:** R = 4-CH<sub>3</sub>OC<sub>6</sub>H<sub>4</sub>  
**7d:** R = 4-FC<sub>6</sub>H<sub>4</sub>  
**7e:** R = 4-BrC<sub>6</sub>H<sub>4</sub>  
**7f:** R = 3-BrC<sub>6</sub>H<sub>4</sub>  
**7g:** R = 2-naphthyl

**8a:** R = C<sub>6</sub>H<sub>5</sub>  
**8b:** R = 4-CH<sub>3</sub>C<sub>6</sub>H<sub>4</sub>  
**8c:** R = 4-CH<sub>3</sub>OC<sub>6</sub>H<sub>4</sub>  
**8d:** R = 4-FC<sub>6</sub>H<sub>4</sub>  
**8e:** R = 4-BrC<sub>6</sub>H<sub>4</sub>  
**8f:** R = 3-BrC<sub>6</sub>H<sub>4</sub>  
**8g:** R = 2-naphthyl

Entry	Catalyst	Substrate	<i>ee</i> [%] <sup>[b]</sup>	Entry	Catalyst	Substrate	<i>ee</i> [%] <sup>[b]</sup>
1	<b>4a</b>	<b>7a</b>	97	13	<b>4c</b>	<b>7b</b>	95
2	<b>4a</b>	<b>7b</b>	93	14	<b>4c</b>	<b>7c</b>	90
3	<b>4a</b>	<b>7c</b>	96	15	<b>4c</b>	<b>7d</b>	95
4	<b>4a</b>	<b>7d</b>	93	16	<b>4c</b>	<b>7e</b>	93
5	<b>4a</b>	<b>7e</b>	95	17	<b>4c</b>	<b>7f</b>	93
6	<b>4a</b>	<b>7g</b>	93	18	<b>4c</b>	<b>7g</b>	90
7	<b>4b</b>	<b>7a</b>	95	19	<b>4d</b>	<b>7a</b>	97
8	<b>4b</b>	<b>7b</b>	95	20	<b>4e</b>	<b>7a</b>	97
9	<b>4b</b>	<b>7c</b>	94	21	<b>4f</b>	<b>7a</b>	98
10	<b>4b</b>	<b>7d</b>	96	22	<b>4g</b>	<b>7a</b>	95
11	<b>4b</b>	<b>7g</b>	90	23	<b>4h</b>	<b>7a</b>	96
12	<b>4c</b>	<b>7a</b>	95	24	<b>4i</b>	<b>7a</b>	93 <sup>[c]</sup>

[a] Conditions:  $[7]=0.2$  M,  $[4]=2$  mM (1 mol% based on the (MonoPhos)<sub>2</sub>/Rh<sup>I</sup> unit),  $T=25^\circ\text{C}$ ,  $P(H_2)=40$  atm,  $t=10$  h, toluene as solvent. Conversion is always >99%. [b] Determined by HPLC (Chiral AD column). [c] (*S*)-**8a** was obtained in this case.

the gentle self-supporting strategy for chiral catalyst immobilization.

Figure 4 shows the reaction profiles for selected self-supported catalysts and comparison to the homogeneous MonoPhos-based system (Rh-**1**<sub>2</sub>) under the same conditions.<sup>[22]</sup> Notably, the catalytic activity observed for **4h** and **4i** (TOF=95 and 97 h<sup>-1</sup> at 2 atm, respectively) is actually higher than that for the homogeneous counterpart.<sup>[23]</sup> Thus, heterogeneous catalyst **4h** yields **6b** in >95% conversion at 60 min (>99% after 90 min) with a constant *ee* value of 97%. Slightly lower reactivities were observed for **4b-g** (TOF range = 71–87 h<sup>-1</sup> at 2 atm), whereas catalyst **4b** re-

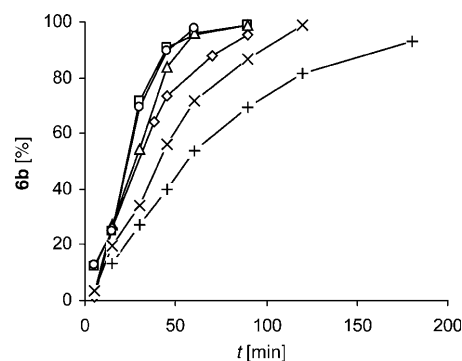


Figure 4. Comparison of the catalytic performance of selected self-supported catalysts (**4**) with homogeneous MonoPhos/Rh in the hydrogenation of **5b** ( $[4]=1$  mM,  $[5b]=0.1$  M,  $P(H_2)=2$  atm,  $T=25^\circ\text{C}$ , toluene as solvent). Key:  $\square=4h$ ;  $\circ=4i$ ;  $\triangle=\text{Rh}^{\text{I}}\text{-1}_2$ ;  $\diamond=4e$ ;  $\times=4g$ ;  $+=4b$ .

quired considerably longer reaction times by comparison ( $\text{TOF} = 51 \text{ h}^{-1}$  at 2 atm). In all cases the obtained enantioselectivity for **6b** was constant for each profile with all catalysts providing product in the range of 95–98% *ee*. This rate enhancement is considered to result from favorable structural changes inherent in the metal–organic polymerization process. For example, effects on ligand rigidity and/or pseudo-bite angle for the two component MonoPhos units about the Rh metal may provide a positive influence on the catalysis. In addition, site isolation due to heterogenization may minimize unwanted saturation of reactive metal centers by irreversible clustering and aggregation during catalysis.<sup>[24]</sup> In fact, for a homogeneous hydrogenation catalyst prepared in situ with  $\text{Rh}^{\text{I}}$  salt and a monophosphorus ligand L, a dynamic mixture of  $\text{Rh}^{\text{I}}$  complexes composed of species such as  $\text{ML}_1$ ,  $\text{ML}_2$ ,  $\text{ML}_3$ , and  $\text{ML}_4$  may exist, among which the  $\text{ML}_2$  species is usually held responsible for the catalysis.<sup>[17c, g, 18]</sup> In the present work, the self-supported catalysts **4a–i** were generated on the basis of the  $\text{ML}_2$  coordination pattern, which seems to fit the structural requirement of the active species. The use of sterically bulky tritopic or tetra-topic ligands **3h** and **3i** to generate a self-supported Rh catalyst can minimize the possibility of forming  $\text{ML}_3$  or  $\text{ML}_4$  species, and this presumably can be one reason why catalysts **4h** and **4i** demonstrated superior catalytic activity over other ditopic-ligand-based catalysts. In any event, the comparable reactivity to analogous homogeneous systems renders the self-supporting approach an outstanding strategy for catalyst immobilization. These results clearly show that modifications in the linker moieties of the bridging ligands may alter the supramolecular structures of the assemblies, and as a result, have an impact on the catalysis. Coupled with the fact that the coordinatively unsaturated reactive metal centers of the resulting polymers remain relatively uncompromised by the self-supporting process, such subtle influences can result in better catalyst performance in terms of enantioselectivity and/or reactivity. Thus, the heterogeneous catalyst may be fine-tuned to optimize the overall catalysis for the reaction of a given substrate, outperforming their homogeneous counterparts as a result.

Hydrogenation by a gas–liquid–solid reaction has the inherent disadvantage of slow mass transfer. Accordingly, the reaction is typically performed under high pressure to minimize such (and related) issues. Alternatively, increasing the interfacial area between gas ( $\text{H}_2$ ), liquid (solvent and substrate), and solid (catalyst) will also result in better reaction rates. For this reason, an understanding of the nature of the self-supported catalyst during hydrogenation is extremely important. Although BET measurements suggest a nonporous material for the present self-assembled metal–organic polymers, this precatalyst condition might very well change in solution under hydrogenation conditions. As observed in a number of polymer (cross-linked) or resin-bound catalyst systems,<sup>[3b, 4a, g, i]</sup> a nonporous polymer would be expected to undergo swelling in the reaction solvent. However, as can be seen in Figure 5, changing the stirring (and mixing) time prior to  $\text{H}_2$  activation did not result in any significant

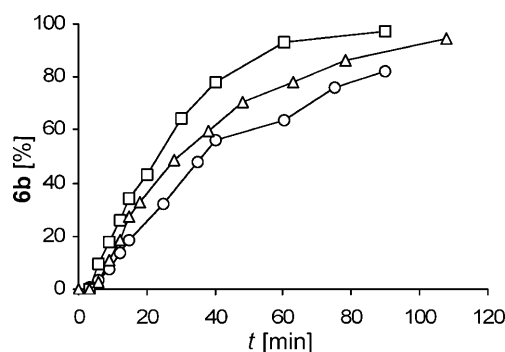


Figure 5. Catalyst **4h** performance in catalyst formation with a variation of stirring time (○ = <math>t < 3 \text{ min}</math>; □ = <math>t = 10 \text{ h}</math>; △ = <math>t = 10 \text{ min}</math>).

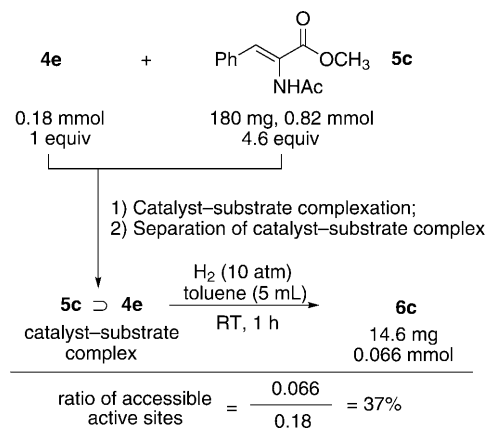
change to the overall reaction profile shape. For a swelling process, notable incubation periods result from limited catalyst turnover due to hidden active sites prior to swelling. Nevertheless, there is a definite difference in the TOF for the differently made precatalysts, with longer precatalyst stirring times resulting in increases in catalyst activity. We consider this to be due to an increase in the overall available surface as a result of mechanical stirring, which causes a reduction in the average particle size (see Figure S1b,c in the Supporting Information). This effect acts in two major ways: 1) it increases direct exposure of active sites on the surface of the catalyst to the substrate, and 2) it increases the availability and access of substrate (solvent) to interstitial active sites within the catalyst/polymer matrix. In addition, it may be expected that polymer units may break and come together during catalysis to similarly expose “new” active sites. This is particularly likely since metal coordination involves nonchelating monodentate ligand types. However, current mechanistic data on analogous homogeneous monodentate P ligands suggest that a 2:1 ligand/Rh complex is involved in the active catalyst. Thus, considering the exceptionally high enantioselectivity obtained with the self-supported catalysts, 2:1 ligand/Rh units should predominate in these systems.

#### Estimation of effective catalytic sites in the self-supported catalyst:

It has been generally accepted that in the  $\text{Rh}^{\text{I}}$ -catalyzed asymmetric hydrogenation of  $\alpha$ -dehydroamino acid derivatives, the active catalyst first reacts with substrate in a pre-equilibrium to form the catalyst–substrate complex. In the rate-determining step, this complex finally reacts to form the product and regenerate the catalyst. The NMR spectroscopic technique and X-ray molecular structure determinations of the catalyst–substrate complexes have provided a wide range of evidence for the formation and the involvement of these species in the catalysis.<sup>[25]</sup> On the basis of this mechanistic understanding, we decided to measure the ratio of accessible active sites in our self-supported  $\text{Rh}^{\text{I}}$  catalysts by isolating the solid-catalyst–substrate complex and performing their hydrogenation. Assuming that the complexed substrate in the solid catalyst can be completely converted to the product in a stoichiometric manner, the amount of the product obtained corresponds to the sum of

catalyst–substrate complex, and thus provides a rough estimation of how much accessible active site is present in the solid catalyst.

As shown in Scheme 3, the self-supported catalyst **4e** (0.18 mmol) was first treated with H<sub>2</sub> (10 atm) to remove the coordinated cycloocta-1,5-diene around the Rh<sup>I</sup> center, and the resultant catalyst was reacted with  $\alpha$ -dehydroamino



Scheme 3. Isolation and hydrogenation of the catalyst–substrate complex for the estimation of effective catalytic sites in the self-supported catalyst **4e**.

acid derivative **5c** (4.6 equiv, 0.82 mmol) in toluene. The mixture was stirred for 1 h and the resulting solid was separated by filtration and washed with toluene (3 × 5 mL) to ensure the complete removal of the uncomplexed **5c**. Finally, the isolated self-supported catalyst (**4e**) saturated by substrate **5c** was recharged with toluene and H<sub>2</sub>; 14.6 mg (0.066 mmol) of hydrogenated product **6c** was obtained with 96% *ee*. Based on these experimental data, it can be deduced that approximately 37% of the Rh<sup>I</sup> centers in the self-supported catalyst **4e** are accessible to the large-size substrate **5c**. This high ratio of effective catalytic sites in the self-supported catalyst may provide a rationale for its relatively high activity in the heterogeneous catalysis.

**Catalyst recycling:** The tremendous advantage of the self-supported heterogeneous catalysts over their homogeneous counterparts, notwithstanding their comparable reactivity and enantioselectivity, was exemplified by the facile recovery and recycling of **4h** during the asymmetric hydrogenation of **5b**. Following the completion of hydrogenation, simple cannula filtration of the reaction mixture under an N<sub>2</sub> atmosphere in a glove box allowed the separation of the solid-state catalyst from the product-containing solution. The isolated solids were recharged with toluene and substrate, and reloaded into the glass autoclave for the next run. Figure 6 shows the reaction profiles for the first and second run for a single reuse ([**4h**] = 1 mM (based on (MonoPhos)<sub>2</sub>/Rh<sup>I</sup> unit), [**5b**] = 0.1 M, P(H<sub>2</sub>) = 2 atm, T = 25 °C, toluene solvent). It is evident that the system experiences a significant drop in the reactivity upon recycling. The TOF for

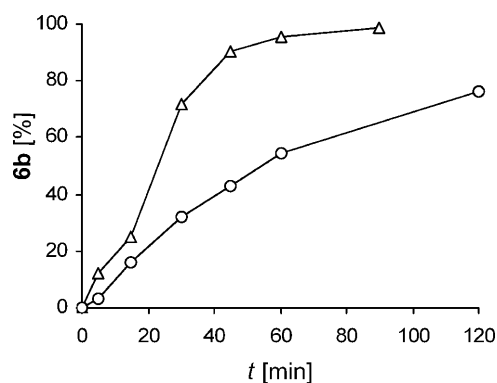


Figure 6. Reaction profiles (Δ=first run; ○=second run) for the recycling of self-supported catalyst **4h** in the hydrogenation of  $\alpha$ -dehydroamino acid derivative **5b**.

the hydrogenation drops from 95 to 54 h<sup>-1</sup> (2 atm) for the first and second run, respectively, however, the enantioselectivity remained the same for both runs (97% *ee*).

Results for an analogous hydrogenation recycled a total of 10 times are given in Table 3. Here, the hydrogenation

Table 3. Determination of turnover frequency (TOF) during recycling of catalyst **4h** for the asymmetric hydrogenation of **5b**.<sup>[a]</sup>

Run	t [min] <sup>[b]</sup>	Conversion [%]	TOF <sup>[c]</sup>	<i>ee</i> [%] <sup>[d]</sup>
1	25	71	170	96
2	30	75	152	95
3	30	72	145	96
4	30	67	135	97
5	40	73	111	97
6	60	85	86	97
7	70	81	69	97
8	90	81	54	97
9	115	81	42	96
10	130	68	31	96

[a] Conditions: [**5b**] = 0.4 M, [**4h**] = 4 mM (1 mol% based on the (MonoPhos)<sub>2</sub>/Rh<sup>I</sup> unit), T = 25 °C, P(H<sub>2</sub>) = 3 atm, toluene as solvent. [b] Reaction was stopped at approximately > 70% conversion. [c] For definition see ref. [21]. [d] Determined by GC (Supelco BETA-DEX 225 column).

was stopped after approximately > 70% conversion so that the TOF could be calculated for each consecutive run. Although no significant loss in enantioselectivity was observed (96–97% *ee*), the TOF for each successive run (recycle) drops by a significant, near-constant amount (ca. 20%). This highlights an important issue when discussing the recyclability of catalysts, since such a drop in reactivity (TOF) may go unnoticed if conversion is used to quantify catalyst activity. This decrease in reactivity with recycling can be attributed to a number of reasons,<sup>[2–4]</sup> some inherent to the method of catalyst immobilization and recycling. Presently, we suggest that partial catalyst decomposition during the recycling process due to instability of intermediate catalyst species might be responsible. Importantly, the leaching of Rh metal in each cycle during recycling of the catalyst was less than 1 ppm, as determined by ICP spectroscopy. Although the presence of adventitious air or moisture cannot be ruled

out, we suggest that the removal of the  $H_2$  atmosphere during recycling is obviously unfavorable for the stability of the catalytically active species. For a set reaction time of 10 h, catalyst **4c** has previously been recycled up to 7 times (here, filtration of the catalyst was carried out using a standard Schlenk technique under an argon atmosphere, but not in a glove box) with quantitative conversion ( $>99\%$ ), but yielding **6a** with a noticeable drop in enantioselectivity (95–89%).<sup>[16c]</sup> This again demonstrated that the instability of intermediate catalyst species is a problematic issue during recycling in the absence of  $H_2$ .

**Development of a continuous flow system:** To further enhance the performance of a heterogeneous catalyst for hydrogenation, various continuous flow reactors have been developed using different strategies for stationary-phase catalyst immobilization.<sup>[26,27]</sup> Such processes offer several advantages over existing batch techniques, particularly when using an anchored catalyst phase.<sup>[28]</sup> Primarily, the reaction parameters like flow rate, system pressure, reaction stoichiometry, and temperature can be readily controlled and monitored, leading to well-defined and reproducible reaction conditions. Moreover, such systems are readily scalable by application of multichannel, parallel reactors, or extended running times. These factors thus allow for a large product-to-catalyst output without the need for repeated catalyst recycling, which typically suffers from a progressive loss in catalyst performance.<sup>[4]</sup> Particularly for the hydrogenation catalyst, the stability may be also enhanced by avoiding the decomposition of unstable metal species during the separation of catalyst in the absence of  $H_2$  atmosphere.

As we mentioned above, a decrease in reactivity with consecutive recycling is a general problem for hydrogenation using immobilized catalysts.<sup>[4]</sup> Accordingly, continuous flow reactors may provide a good opportunity to overcome this limitation and improve overall process capacity and productivity.<sup>[26–28]</sup> On the other hand, the high TOF of the self-supported MonoPhos/Rh catalyst system in batch heterogeneous hydrogenation can meet the basic requirement for the development of a continuous flow reaction system due to the short interaction time between immobilized catalyst and flowing substrate in the flow reaction system. Presently, a continuous flow reactor was designed and developed for asymmetric hydrogenation using the self-supporting strategy for stationary-phase catalyst immobilization. The principle design elements are illustrated in Figure 7. The reactor setup allows for a continuous flow of the substrate solution and hydrogen gas through a tube reactor packed with the heterogenized catalyst. The gas–liquid mixture is pumped through a T-shaped mixer to ensure efficient gas dispersion, while the flow of the substrate solution was controlled by an HPLC pump and the flow of the hydrogen gas was regulated by a gas flow controller. The mixed hydrogen–substrate solution flow stream formed within the T-shaped cross was driven to flow continuously through a 4.6 mm inner diameter and 2 cm stainless steel column that was prepacked with the solid catalyst. At the outlet of the column, the product

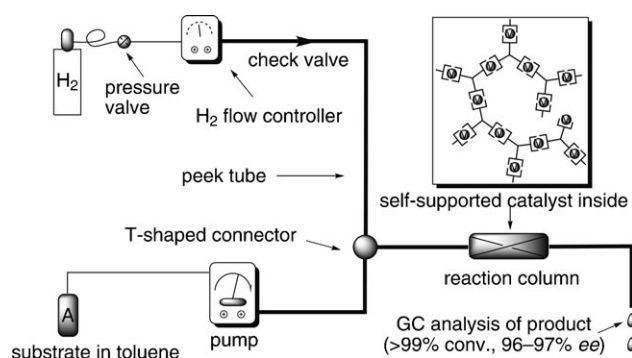


Figure 7. Schematic representation of the continuous flow reactor using self-supported catalyst.

solution was collected for GC analysis and the excess amount of the hydrogen gas came out at atmospheric pressure.

Initially, self-supported catalyst **4b** was packed into the column and used as the stationary heterogeneous catalyst phase. However, use of this metal–organic polymer alone or a **4b**/ $MgSO_4$  (with an average diameter of  $15\ \mu m$ ) (120 mg/170 mg) mixture quickly resulted in system blockage. Increasing the loading of the inorganic salt (**4b**/ $MgSO_4$  = 60 mg/230 mg) allowed for the flow system to function continuously following an initial stabilization period (ca. 3 h). Under standardized conditions (**4b** = 60 mg,  $MgSO_4$  = 230 mg; [**5b**] = 1 g/100 mL; flow rate = 0.1 or 0.05 mL  $min^{-1}$ ;  $H_2$  flow rate = 3 mL  $min^{-1}$ ; toluene as solvent), the conversion could be continuously maintained at 55–76% for a period of 52 h, yielding product **6b** in 94–96% *ee*. However, possibly due to temporary blockage of the continuous flow, the pressure for this system was observed to be unstable.

To improve the productivity and flow properties of the packed column, other packing materials were tested. Reaction profiles under the same standard conditions for heterogeneous asymmetric hydrogenation of **5b** by catalysts comprised of **4b** and  $MgSO_4$ ,  $TiO_2$  (with an average diameter of  $0.1\ \mu m$  and a specific surface area of  $90\ m^2\ g^{-1}$ ), or activated carbon (with an average diameter of  $30\ \mu m$  and a specific surface area of  $1000\ m^2\ g^{-1}$ ) are shown in Figure 8. The **4b**/

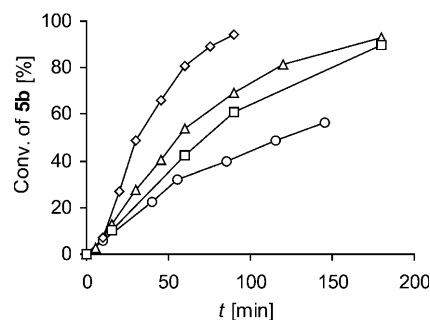


Figure 8. Reaction profiles for mixtures of **4b** with added support ( $\Delta$  = no support;  $\circ$  =  $TiO_2$ ;  $\square$  =  $MgSO_4$ ;  $\diamond$  = carbon) under the following conditions: [**4b**] = 1 mM, [**5b**] = 0.1 M,  $P(H_2)$  = 2 atm,  $T$  = 25 °C, toluene as solvent.

MgSO<sub>4</sub> system shows slightly lower but comparable reactivity to **4b** alone, whereas mixing with TiO<sub>2</sub> clearly results in a less active catalyst. Most notably, the reactivity when activated carbon was used as added support significantly increased the reactivity beyond that of the self-supported catalyst **4b** alone. This is somewhat surprising but may be attributable to the improved dispersion of **4b** in the reaction mixture in the presence of activated carbon. For all systems, however, the obtained enantioselectivity in **6b** for mixed systems is relatively constant (96–97% *ee*) when compared to **4b** alone (97% *ee*) or the homogeneous **1**–Rh catalyst (97% *ee*). This indicates that the delicate local multitopic ligand/Rh metal electronic and steric properties are not influenced by the addition of an added support.

Since reaction profiles (see Figure 4) of the various heterogenized catalysts (**4**) showed that **4h** and **4i** give an outstanding result both in activity and enantioselectivity, even under low H<sub>2</sub> pressure (2 atm), **4h** was selected for catalyst column loading because of its easy preparation. (For SEM images of **4h**, activated carbon, the mixture of catalyst **4h**, and activated carbon, see Figures S1a and S1d in the Supporting Information.) Under the experimental conditions, product **6b** could be continuously obtained in >99% conversion (93–94 μmol h<sup>-1</sup>) in 97% *ee* for a total of 144 h (Figure 9). This corresponds to a constant daily production of 0.36 g (2.25 mmol), giving an overall yield of 2.52 g (15.75 mmol) of **6b** after 144 h. The leaching of Rh into the product solution in toluene was 0.13 ppm, corresponding to 1.7% of that in the original catalyst **4h** (determined by ICP spectroscopy). Thus, the self-supporting strategy provides a viable means for chiral catalyst immobilization in continuous flow reactors.

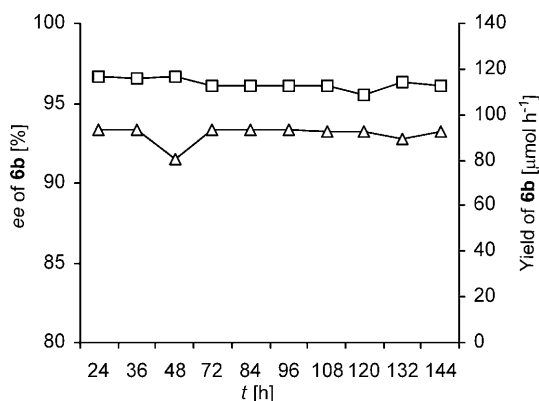


Figure 9. Catalytic performance (□ = *ee*; Δ = yield) of the continuous flow reactor in the asymmetric hydrogenation of **5b** (reaction column: 4.6 mm inner diameter and 2 cm in length; **4h** = 60 mg; activated carbon = 90 mg; reaction conditions: [**5b**] = 1 g/200 mL, flow rate = 0.05 mL min<sup>-1</sup>, H<sub>2</sub> flow rate = 3 mL min<sup>-1</sup>, toluene as solvent).

## Conclusion

Construction of self-assembled metal–organic frameworks using well-designed multitopic ligands and reactive metal

centers comprises a simple and efficient means of chiral catalyst immobilization. The resulting self-supported catalysts are stable and well behaved under catalytic conditions; they show outstanding reactivity and selectivity, comparable to or even better than their analogous homogeneous counterparts. Variation of the linker (or spacer) adjoining the coordinating groups allows for fine-tuning of the catalytic performance. The resultant homochiral metal–organic coordination polymers are easily recycled without significant loss in enantioselectivity, although a drop in reactivity is apparent. The latter can be overcome by employment of a continuous flow reactor, which allows for high efficiency for extended periods without loss in reactivity or enantioselectivity. Thus, the self-supported approach is a reliable (and general) method for immobilization of MonoPhos/Rh catalyst in asymmetric hydrogenation. The immobilized catalyst is applicable in both batch recycling and continuous flow processes, constituting a very competitive heterogenization strategy in asymmetric catalysis.

## Experimental Section

All the experiments sensitive to moisture or air were carried out under an argon atmosphere using standard Schlenk techniques. Dichloromethane and chloroform were freshly distilled from calcium hydride; and THF, diethyl ether, and toluene from sodium benzophenone ketyl. Commercial reagents were used as received without further purification unless otherwise noted. Compounds **2a–c**,<sup>[16c]</sup> **2d–i**,<sup>[13a]</sup> **3a–c**,<sup>[16c]</sup> and **4a–c**<sup>[16c]</sup> were prepared as previously reported.

<sup>1</sup>H NMR and <sup>13</sup>C NMR spectroscopy were conducted using a Varian Mercury 300 (<sup>1</sup>H: 300 MHz; <sup>13</sup>C: 75 MHz) spectrometer. Chemical shifts are reported in ppm relative to the internal standard Si(CH<sub>3</sub>)<sub>4</sub> (δ = 0.0 ppm) for <sup>1</sup>H NMR spectroscopy and CDCl<sub>3</sub> (δ = 77.0 ppm) for <sup>13</sup>C NMR spectroscopy. Coupling constants, *J*, are listed in Hertz. <sup>31</sup>P NMR spectra were referenced with an external 85% H<sub>3</sub>PO<sub>4</sub> sample. <sup>31</sup>P NMR CP-MAS spectra were measured using a Bruker DSX300 NMR spectrometer (125 MHz). Chemical shifts were referenced from 70% H<sub>3</sub>PO<sub>4</sub> (δ = 0.0 ppm) as external standard. EI (70 eV) and ESI mass spectra (MS) were conducted using HP5989A and Mariner LC-TOF spectrometers, respectively. HRMS spectra were determined using a Q-ToF micro instrument or APEXIII 7.0 TESLA FTMS. Elemental analysis was performed using an Elemental VARIO EL apparatus. Optical rotations were measured using a Perkin–Elmer 341 automatic polarimeter. Infrared (IR) spectra were obtained using a BIO-RAD FTS-185 Fourier transform spectrometer using KBr pellets. Scanning electron micrographs were taken using a Hitachi S-570 scanning electron microscope. Powder X-ray diffraction (XRD) spectroscopy was conducted using a Bruker-AXS D8 Advance spectrometer. ICP analysis was performed using a Varian spectra AA. Liquid chromatographic (LC) analyses were conducted using a JASCO 1580 system. GC analyses were conducted using an Agilent 6890N network system.

**General procedure for the synthesis of compounds 3d–i:** The corresponding bis-BINOL (**2**) derivative (1.0 mmol) and hexamethylphosphorous triamide (0.46 mL, 2.5 mmol) were heated at reflux for 9 h in anhydrous toluene (3.0 mL) under an argon atmosphere. After cooling to room temperature, the solvent was removed under reduced pressure and the crude pale yellow residue was purified by flash chromatography on silica gel using petroleum ether/ethyl acetate (10:1) for **3d–h** or petroleum ether/dichloromethane (2:1) for **3i** as eluent. Recrystallization from diethyl ether afforded pure product as a white (**3d–g, i**) or pale yellow (**3h**) solid.

**Compound 3d:** Yield: 526 mg (76%); m.p. 164–167 °C; [ $\alpha$ ]<sub>D</sub><sup>20</sup> = +620.7 (*c* = 0.5 in CHCl<sub>3</sub>); <sup>1</sup>H NMR (300 MHz, CDCl<sub>3</sub>): δ = 8.14 (d, *J* = 3.0 Hz,

2H), 7.87–7.99 (m, 6H), 7.49–7.53 (m, 2H), 7.29–7.45 (m, 12H), 2.53–2.57 ppm (m, 12H);  $^{31}\text{P}$  NMR (121 MHz,  $\text{CDCl}_3$ ):  $\delta$  = 149.98, 150.06 ppm; FTIR (KBr pellet):  $\tilde{\nu}$  = 3055, 2964, 2922, 2844, 2800, 2205, 1619, 1589, 1506, 1469, 1461, 1361, 1334, 1292, 1262, 1233, 1207, 1187, 1072, 1027, 984, 944, 922, 888, 836, 820, 796, 791, 780, 749, 693, 677, 637  $\text{cm}^{-1}$ ; MS (MALDI-DHB):  $m/z$ : 741.20  $[\text{M}+\text{H}]^+$ ; HRMS (MALDI-DHB):  $m/z$ : calcd for  $\text{C}_{46}\text{H}_{35}\text{N}_2\text{O}_4\text{P}_2$   $[\text{M}+\text{H}]^+$ : 741.2066; found: 741.2093.

**Compound 3e:** Yield: 621 mg (74%); m.p. 169–172 °C;  $[\alpha]_{\text{D}}^{20}$  = +610.2 ( $c$  = 0.5 in  $\text{CHCl}_3$ );  $^1\text{H}$  NMR (300 MHz,  $\text{CDCl}_3$ ):  $\delta$  = 8.13 (d,  $J$  = 3.3 Hz, 2H), 7.86–7.99 (m, 6H), 7.54 (s, 4H), 7.25–7.52 (m, 14H), 2.53–2.57 ppm (m, 12H);  $^{31}\text{P}$  NMR (121 MHz,  $\text{CDCl}_3$ ):  $\delta$  = 149.98, 150.10 ppm. FTIR (KBr pellet):  $\tilde{\nu}$  = 3057, 2922, 2845, 2800, 2202, 1588, 1509, 1463, 1334, 1292, 1234, 1207, 1188, 1070, 984, 944, 913, 888, 836, 820, 796, 790, 751, 693, 677, 635  $\text{cm}^{-1}$ ; MS (MALDI-DHB):  $m/z$ : 840.20  $[\text{M}]^+$ ; HRMS (MALDI-DHB):  $m/z$ : calcd for  $\text{C}_{54}\text{H}_{39}\text{N}_2\text{O}_4\text{P}_2$   $[\text{M}+\text{H}]^+$ : 841.2379; found: 841.2385.

**Compound 3f:** Yield: 663 mg (79%); m.p. 214–217 °C;  $[\alpha]_{\text{D}}^{20}$  = +597.4 ( $c$  = 0.5 in  $\text{CHCl}_3$ );  $^1\text{H}$  NMR (300 MHz,  $\text{CDCl}_3$ ):  $\delta$  = 8.13 (d,  $J$  = 3.3 Hz, 2H), 7.90–7.96 (m, 6H), 7.76 (s, 1H), 7.49–7.54 (m, 4H), 7.25–7.45 (m, 13H), 2.53–2.57 ppm (m, 12H);  $^{31}\text{P}$  NMR (121 MHz,  $\text{CDCl}_3$ ):  $\delta$  = 150.02, 150.11 ppm; FTIR (KBr pellet):  $\tilde{\nu}$  = 3057, 2953, 2924, 2845, 2800, 2207, 1591, 1506, 1463, 1334, 1293, 1233, 1207, 1188, 1071, 984, 945, 889, 822, 790, 750, 694, 637  $\text{cm}^{-1}$ ; MS (MALDI-DHB):  $m/z$ : 841.10  $[\text{M}+\text{H}]^+$ ; HRMS (MALDI-DHB):  $m/z$ : calcd for  $\text{C}_{54}\text{H}_{39}\text{N}_2\text{O}_4\text{P}_2$   $[\text{M}+\text{H}]^+$ : 841.2379; found: 841.2378.

**Compound 3g:** Yield: 537 mg (64%); m.p. 210–213 °C;  $[\alpha]_{\text{D}}^{20}$  = +679.5 ( $c$  = 0.5 in  $\text{CHCl}_3$ );  $^1\text{H}$  NMR (300 MHz,  $\text{CDCl}_3$ ):  $\delta$  = 8.17 (d,  $J$  = 9.9 Hz, 2H), 7.90–7.99 (m, 4H), 7.67–7.79 (m, 2H), 7.58–7.61 (m, 2H), 7.23–7.52 (m, 16H), 2.53–2.56 ppm (m, 12H);  $^{31}\text{P}$  NMR (121 MHz,  $\text{CDCl}_3$ ):  $\delta$  = 149.92, 150.09 ppm; FTIR (KBr pellet):  $\tilde{\nu}$  = 3056, 2923, 2845, 2801, 2199, 1619, 1587, 1505, 1462, 1355, 1334, 1294, 1230, 1207, 1070, 985, 944, 822, 790, 756, 694, 636  $\text{cm}^{-1}$ ; MS (MALDI-DHB):  $m/z$ : 841.10  $[\text{M}+\text{H}]^+$ ; HRMS (MALDI-DHB):  $m/z$ : calcd for  $\text{C}_{54}\text{H}_{39}\text{N}_2\text{O}_4\text{P}_2$   $[\text{M}+\text{H}]^+$ : 841.2379; found: 841.2383.

**Compound 3h:** Yield: 855 mg (70%); m.p. 279–281 °C;  $[\alpha]_{\text{D}}^{20}$  = +614.2 ( $c$  = 0.5 in  $\text{CHCl}_3$ );  $^1\text{H}$  NMR (300 MHz,  $\text{CDCl}_3$ ):  $\delta$  = 8.13 (d,  $J$  = 3.6 Hz, 3H), 7.87–7.99 (m, 10H), 7.70 (s, 2H), 7.27–7.54 (m, 22H), 2.52–2.58 ppm (m, 18H);  $^{31}\text{P}$  NMR (121 MHz,  $\text{CDCl}_3$ ):  $\delta$  = 150.00, 150.11 ppm;  $^{31}\text{P}$  NMR CP-MAS:  $\delta$  = 148.80 ppm; FTIR (KBr pellet):  $\tilde{\nu}$  = 3055, 2922, 2887, 2844, 2800, 2208, 1619, 1589, 1506, 1469, 1332, 1293, 1233, 1207, 1188, 1071, 983, 945, 887, 829, 796, 790, 780, 749, 693, 648  $\text{cm}^{-1}$ ; MS (MALDI-DHB):  $m/z$ : 1222.30  $[\text{M}+\text{H}]^+$ ; HRMS (MALDI-DHB):  $m/z$ : calcd for  $\text{C}_{78}\text{H}_{55}\text{N}_3\text{O}_6\text{P}_3$   $[\text{M}+\text{H}]^+$ : 1222.3298; found: 1222.3294.

**Compound 3i:** Yield: 1277 mg (65%); m.p. > 310 °C;  $[\alpha]_{\text{D}}^{20}$  = –271.7 ( $c$  = 0.5 in DMF);  $^1\text{H}$  NMR (300 MHz,  $\text{CDCl}_3$ ):  $\delta$  = 8.12 (d,  $J$  = 2.4 Hz, 4H), 7.85–7.98 (m, 12H), 7.23–7.57 (m, 44H), 2.52–2.58 (m, 24H), 2.18 ppm (s, 12H);  $^{31}\text{P}$  NMR (121 MHz,  $\text{CDCl}_3$ ):  $\delta$  = 150.09, 150.16 ppm;  $^{31}\text{P}$  NMR CP-MAS:  $\delta$  = 148.75 ppm; FTIR (KBr pellet):  $\tilde{\nu}$  = 3055, 2922, 2887, 2844, 2800, 2208, 1619, 1589, 1506, 1469, 1332, 1293, 1233, 1207, 1188, 1071, 983, 945, 887, 829, 796, 790, 780, 749, 693, 648  $\text{cm}^{-1}$ ; MS (MALDI-DHB):  $m/z$ : 1920.5  $[\text{M}-\text{NMe}_2]^+$ ; HRMS (MALDI-DHB):  $m/z$ : calcd for  $\text{C}_{128}\text{H}_{90}\text{N}_5\text{O}_8\text{P}_4$   $[\text{M}-\text{NMe}_2]^+$ : 1920.5672; found: 1920.5726.

**General procedure for the synthesis of catalysts 4d–i:** Compound **3** (a–g) (0.011 mmol), **3h** (0.0073 mmol), or **3i** (0.0055 mmol) in dichloromethane (1.0 mL) was added to a solution of  $[\text{Rh}(\text{cod})_2]\text{BF}_4$  (4.06 mg, 0.01 mmol) in dichloromethane (0.5 mL). The solution was stirred at room temperature for 30 min, ultimately affording an orange precipitate. After removal of the solvents at 50 °C under reduced pressure, the residue was dried in vacuo (2 h). The resulting orange powder was washed with toluene to remove any trace amount of soluble low molecular weight species to give **4**.

**Compound 4d:** FTIR (KBr pellet):  $\tilde{\nu}$  = 2924, 2853, 1620, 1590, 1508, 1465, 1432, 1361, 1261, 1226, 1178, 1072, 1009, 990, 964, 947, 865, 827, 687, 590  $\text{cm}^{-1}$ ; elemental analysis calcd (%) for  $[\text{Rh}(\text{cod})(\mathbf{3d})]\text{BF}_4\cdot\text{CH}_2\text{Cl}_2\cdot n$ : C 58.8, H 4.31, N 2.49; found: C 59.43, H 5.18, N 2.07.

**Compound 4e:** FTIR (KBr pellet):  $\tilde{\nu}$  = 2924, 2855, 1621, 1589, 1508, 1464, 1328, 1261, 1226, 1071, 990, 948, 864, 699, 569  $\text{cm}^{-1}$ ; elemental analysis

calcd (%) for  $[\text{Rh}(\text{cod})(\mathbf{3e})]\text{BF}_4\cdot\text{CH}_2\text{Cl}_2\cdot n$ : C 61.84, H 4.28, N 2.29; found: C 61.77, H 5.08, N 1.90.

**Compound 4f:** FTIR (KBr pellet):  $\tilde{\nu}$  = 2924, 1620, 1591, 1508, 1464, 1330, 1262, 1226, 1178, 1157, 1070, 989, 964, 946, 890, 828, 791, 752, 698, 581  $\text{cm}^{-1}$ ; elemental analysis calcd (%) for  $[\text{Rh}(\text{cod})(\mathbf{3f})]\text{BF}_4\cdot n$ : C 65.39, H 4.43, N 2.46; found: C 65.79, H 5.69, N 2.01.

**Compound 4g:** FTIR (KBr pellet):  $\tilde{\nu}$  = 3061, 2925, 1621, 1590, 1508, 1463, 1328, 1261, 1226, 1179, 1071, 1008, 990, 948, 864, 828, 791, 753, 699, 662, 587  $\text{cm}^{-1}$ ; elemental analysis calcd (%) for  $[\text{Rh}(\text{cod})(\mathbf{3g})]\text{BF}_4\cdot n$ : C 65.39, H 4.43, N 2.46; found: C 64.45, H 5.39, N 2.01.

**Compound 4h:**  $^{31}\text{P}$  NMR CP-MAS:  $\delta$  = 137.30 ppm; FTIR (KBr pellet):  $\tilde{\nu}$  = 3443, 2923, 2852, 1619, 1589, 1466, 1327, 1226, 1180, 1083, 987, 947, 828, 744, 692  $\text{cm}^{-1}$ ; elemental analysis calcd (%) for  $([\text{Rh}(\text{cod})(\mathbf{3h})]\text{BF}_4)_{1.5}\cdot(\text{CH}_2\text{Cl}_2)_2\cdot n$ : C 60.09, H 4.17, N 2.29, Rh 8.39; found: C 60.05, H 4.61, N 2.14, Rh 7.77.

**Compound 4i:**  $^{31}\text{P}$  NMR CP-MAS:  $\delta$  = 137.04 ppm; FTIR (KBr pellet):  $\tilde{\nu}$  = 3430, 2930, 1589, 1513, 1465, 1336, 1226, 1070, 948, 828, 756, 697, 592  $\text{cm}^{-1}$ ; elemental analysis calcd (%) for  $([\text{Rh}(\text{cod})(\mathbf{3i})]\text{BF}_4)_2\cdot(\text{CH}_2\text{Cl}_2)_3\cdot n$ : C 63.60, H 4.63, N 1.98; found: C 63.09, H 5.00, N 1.91.

**Representative hydrogenation procedure:** Self-supported catalyst **4d** (0.01 mmol based on [Rh] unit) was placed in toluene (5 mL, 2 mm) under an argon atmosphere and stirred for 3 h. To this mixture was then added **5a** (1 mmol) under an argon atmosphere. The test tube was transferred into a stainless steel autoclave that was then sealed. After purging with hydrogen (3 times), the  $\text{H}_2$  pressure was adjusted to 40 atm and stirring commenced. Following the designated reaction time (10 h), the  $\text{H}_2$  was released to stop hydrogenation. The product was obtained by chromatography (petroleum ether/ethyl acetate, 2:1 v/v), followed by the removal of solvents under reduced pressure. Conversion was determined by  $^1\text{H}$  NMR spectroscopy and enantiomeric excess (*ee*) values were determined by chiral GC (Supelco BETA-DEX225 column) or chiral HPLC (Chiralcel AD column).

**Recycling experiments:** Polymeric solid **4h** (0.02 mmol based on [Rh]) was placed in toluene (2.5 mL) under an argon atmosphere and stirred for 3 h. To this mixture was then added a solution of **5b** (2 mmol, 2.5 mL, 0.8 M) in toluene under an argon atmosphere. The test tube was transferred into a stainless steel autoclave that was then sealed. After purging with hydrogen (3 times), the  $\text{H}_2$  pressure was adjusted to 3 atm and stirring commenced. Following a calculated reaction time during which > 70% conversion had been reached, the  $\text{H}_2$  was slowly released. The product and the solid catalyst were separated by cannula filtration under an argon atmosphere. The autoclave was recharged with a new batch of **5b** (2 mmol, 5 mL, 0.4 M) in toluene, purged with hydrogen (3 times), the  $\text{H}_2$  pressure was adjusted to 3 atm, and stirring commenced. This procedure was repeated 9 times (10 cycles). Conversion was determined by  $^1\text{H}$  NMR spectroscopy and enantiomeric excess (*ee*) values were determined by chiral GC (Supelco BETA-DEX225 column). The data are given in Table 3.

**Representative procedure for reaction profile measurement:** Self-supported catalyst **4d** (0.005 mmol based on [Rh] unit) and anhydrous toluene (5.0 mL, 1 mm) were added to a glass autoclave equipped with a sampling needle and a magnetic stirrer bar under an argon atmosphere. The mixture was stirred for at least 3 h. Substrate (**5b**, 0.5 mmol) was then introduced into the autoclave under an argon atmosphere. Following purging with  $\text{H}_2$  (3 times), the pressure was adjusted to 2 atm and stirring commenced ( $t$  = 0 min). Sample aliquots were taken at regular intervals. Conversion and enantiomeric excess (*ee*) values were determined by GC (Supelco BETA-DEX225 column).  $^1\text{H}$  NMR spectral analysis was used to double-check the conversion for each sample aliquot.

**With a different catalyst:** The same conditions were used for each self-supported catalyst: **[4h]** = 1 mm, **[5b]** = 0.1 M,  $P(\text{H}_2)$  = 2 atm,  $T$  = 25 °C, toluene solvent (5 mL). Data are given in Figure 4.

**With different added supports:** a) Carbon: **4b** = 6 mg, activated C = 10 mg, **[5b]** = 0.1 M,  $P(\text{H}_2)$  = 2 atm,  $T$  = 25 °C, toluene solvent (5 mL); b)  $\text{MgSO}_4$ : **4b** = 6 mg,  $\text{MgSO}_4$  = 20 mg, **[5b]** = 0.1 M,  $P(\text{H}_2)$  = 2 atm,  $T$  = 25 °C, toluene solvent (5 mL); c)  $\text{TiO}_2$ : **4b** = 6 mg,  $\text{TiO}_2$  = 20 mg, **[5b]** = 0.1 M,  $P(\text{H}_2)$  =

2 atm,  $T=25^{\circ}\text{C}$ , toluene solvent (5 mL). All these data are given in Figure 8.

**Swelling experiments:** [4h] = 1 mm, [5b] = 0.1 M,  $P(\text{H}_2) = 2$  atm,  $T = 25^{\circ}\text{C}$ , toluene solvent (5 mL). Self-supported catalyst 4 h (0.005 mmol based on [Rh], 1 mm) was placed in toluene (5 mL) under an argon atmosphere and stirred for a designated time prior to use as precatalyst in hydrogenation. Data are given in Figure 5.

#### Continuous flow system

**Typical mixing strategy for packing the catalysts and the support material:** a) After being heated at  $100^{\circ}\text{C}$  under vacuo for 10 h and cooled down to RT, the activated carbon (90 mg) was mixed with catalyst 4h (60 mg) in anhydrous toluene (5 mL) in a container in a glove box. The mixture was stirred at RT for 10 h, and the resulting slurry was introduced using a syringe into a stainless steel tube (4.6 mm inner diameter, 2 cm length) with a filter at one end. The solvent was vacuumed with a pump. After completion, the column was capped with another filter and mounted onto the reaction setup. b) The substrate (5b) solution was mixed with the hydrogen gas in the T-shaped mixer. To maintain this condition, at the inlet of the column, the flow of the substrate solution was controlled to  $0.05\text{ mL min}^{-1}$  by an HPLC pump and the flow of the hydrogen gas was adjusted to  $3.0\text{ mL min}^{-1}$  using a gas mass-flow controller. This resulted in an overall system pressure of 3 atm. At the outlet of the column, the product solution and the excess amount of the hydrogen gas came out at atmospheric pressure. Therefore, the pressure drop between the inlet and the outlet of the column was 2 atm. The product was analyzed by chiral GC (Supelco BETA-DEX225 column) to determine the conversion of the substrate and enantiomeric excess (*ee*) values of the product.  $^1\text{H NMR}$  spectral analysis was used to double-check the conversion.

### Acknowledgements

Financial support from the National Natural Science Foundation of China (nos. 20532050, 20632060, 20620140429), the Chinese Academy of Sciences, the Major Basic Research Development Program of China (grant no. 2006CB806106), the Science and Technology Commission of Shanghai Municipality, and Merck Research Laboratories are gratefully acknowledged.

- [1] a) T. Ohkuma, R. Noyori in *Comprehensive Asymmetric Catalysis, Vol. 1* (Eds.: E. N. Jacobsen, A. Pfaltz, H. Yamamoto), Springer, Berlin, 1999, pp. 199–246; b) T. Ohkuma, M. Kitamura, R. Noyori in *Catalytic Asymmetric Synthesis*, 2nd ed. (Ed.: I. Ojima), Wiley-VCH, Weinheim, 2000, pp. 1–110; c) J. M. Brown in *Comprehensive Asymmetric Catalysis, Vol. 1* (Eds.: E. N. Jacobsen, A. Pfaltz, H. Yamamoto), Springer, Berlin, 1999, pp. 119–182; d) T. Ohkuma, R. Noyori in *Transition Metals for Organic Synthesis, Vol. 2* (Eds.: M. Beller, C. Bolm), Wiley, New York, 1998, pp. 25–69; e) *The Handbook of Homogeneous Hydrogenation* (Eds.: J. G. de Vries, C. J. Elsevier), Wiley-VCH, Weinheim, 2007; f) H.-U. Blaser, R. Hanreich, H.-D. Schneider, F. Spindler, B. Steinacher in *Asymmetric Catalysis on Industrial Scale* (Eds.: H.-U. Blaser, E. Schmidt), Wiley-VCH, Weinheim, 2004, p. 55–70; g) W. S. Knowles, *Angew. Chem.* 2002, 114, 2096–2107; *Angew. Chem. Int. Ed.* 2002, 41, 1998–2007; h) R. Noyori, *Angew. Chem.* 2002, 114, 2108–2123; *Angew. Chem. Int. Ed.* 2002, 41, 2008–2022; i) H.-U. Blaser, C. Malan, B. Pugin, F. Spindler, H. Steiner, M. Studer, *Adv. Synth. Catal.* 2003, 345, 103–151.
- [2] a) *Chiral Catalyst Immobilization and Recycling* (Eds.: D. E. de Vos, I. F. Vankleecom, P. A. Jacobs), Wiley-VCH, Weinheim, 2000; b) *Handbook of Asymmetric Heterogeneous Catalysis* (Eds.: K. Ding, Y. Uozumi), Wiley-VCH, Weinheim, 2008; c) For special issues on recoverable catalysts and reagents, see: *Chem. Rev.* 2002, 102, 3215–3892; d) *Chem. Rev.* 2009, 109, 257–838.
- [3] a) C. Saluzzo, M. Lemaire, *Adv. Synth. Catal.* 2002, 344, 915–928; b) P. Barbaro, *Chem. Eur. J.* 2006, 12, 5666–5675; c) R. Somanathan, N. A. Cortez, M. Parra-Hake, D. Chavez, G. Aguirre, *Mini-Rev. Org. Chem.* 2008, 5, 313–322.
- [4] a) C. Saluzzo, R. terHalle, F. Touchard, F. Fache, E. Schulz, M. Lemaire, *J. Organomet. Chem.* 2000, 603, 30–39; b) C. Bianchini, P. Barbaro, *Top. Catal.* 2002, 19, 17–32; c) S. Bräse, F. Lauterwasser, R. E. Ziegert, *Adv. Synth. Catal.* 2003, 345, 869–929; d) P. Mastrorilli, C. F. Nobile, *Coord. Chem. Rev.* 2004, 248, 377–395; e) P. McMorn, G. J. Hutchings, *Chem. Soc. Rev.* 2004, 33, 108–122; f) C. E. Song, *Annu. Rep. Prog. Chem. Sect. C* 2005, 101, 143–173; g) B. M. L. Dooos, I. V. J. Vankleecom, P. A. Jacobs, *Adv. Synth. Catal.* 2006, 348, 1413–1446; h) D. E. Bergbreiter, S. D. Sung, *Adv. Synth. Catal.* 2006, 348, 1352–1366; i) M. Heitbaum, F. Glorius, I. Escher, *Angew. Chem.* 2006, 118, 4850–4881; *Angew. Chem. Int. Ed.* 2006, 45, 4732–4762.
- [5] For reviews with selected examples therein, see: a) C. Li, *Catal. Rev. Sci. Eng.* 2004, 46, 419–492; b) C. E. Song, D. H. Kim, D. S. Choi, *Eur. J. Inorg. Chem.* 2006, 2927–2935; c) C. Li, H. D. Zhang, D. M. Jiang, Q. H. Yang, *Chem. Commun.* 2007, 547–558; d) J. M. Thomas, R. Raja, *Acc. Chem. Res.* 2008, 41, 708–720. See also ref. [4e].
- [6] For reviews, see: a) L.-X. Dai, *Angew. Chem.* 2004, 116, 5846–5850; *Angew. Chem. Int. Ed.* 2004, 43, 5726–5729; b) K. Ding, Z. Wang, X. Wang, Y. Liang, X. Wang, *Chem. Eur. J.* 2006, 12, 5188–5197; c) L. Shi, Z. Wang, X. Wang, M. Li, K. Ding, *Chin. J. Org. Chem.* 2006, 26, 1444–1456; d) K. Ding, Z. Wang, L. Shi, *Pure Appl. Chem.* 2007, 79, 1531–1538; e) Z. Wang, G. Chen, K. Ding, *Chem. Rev.* 2009, 109, 322–359.
- [7] For reviews, see: a) S. L. James, *Chem. Soc. Rev.* 2003, 32, 276–288; b) S. Kitagawa, R. Kitaura, S. Noro, *Angew. Chem.* 2004, 116, 2388–2430; *Angew. Chem. Int. Ed.* 2004, 43, 2334–2375; c) O. M. Yaghi, M. O’Keeffe, N. W. Ockwig, H. K. Chae, M. Eddaoudi, J. Kim, *Nature* 2003, 423, 705–714; d) A. Y. Robin, K. M. Fromm, *Coord. Chem. Rev.* 2006, 250, 2127–2157; e) G. Férey, *Chem. Soc. Rev.* 2008, 37, 191–214.
- [8] For reviews, see: a) C. Janiak, *Dalton Trans.* 2003, 2781–2804; b) P. M. Forster, A. K. Cheetham, *Top. Catal.* 2003, 24, 79–86; c) F. Schuth, *Annu. Rev. Mater. Res.* 2005, 35, 209–238; d) W. Lin, *J. Solid State Chem.* 2005, 178, 2486–2490.
- [9] For selected examples, see: a) A. Efraty, I. Feinstein, *Inorg. Chem.* 1982, 21, 3115–3118; b) R. Tannenbaum, *Chem. Mater.* 1994, 6, 550–555; c) M. Fujita, Y. J. Kwon, S. Washizu, K. Ogura, *J. Am. Chem. Soc.* 1994, 116, 1151–1152; d) T. Sawaki, T. Dewa, Y. Aoyama, *J. Am. Chem. Soc.* 1998, 120, 8539–8540; e) S. Naito, T. Tanibe, E. Saito, T. Miyao, W. Mori, *Chem. Lett.* 2001, 1178–1179; f) J. M. Tanski, P. T. Wolczanski, *Inorg. Chem.* 2001, 40, 2026–2033; g) B. Gomez-Lor, E. Gutierrez-Puebla, M. A. Monge, C. Ruiz-Valero, N. Snejko, *Inorg. Chem.* 2002, 41, 2429–2432; h) J. Perles, M. Iglesias, C. Ruiz-Valero, N. Snejko, *Chem. Commun.* 2003, 346–347; i) S. K. Yoo, J. Y. Ryu, J. Y. Lee, C. Kim, S. J. Kim, Y. Kim, *Dalton Trans.* 2003, 1454–1456; j) K. Schlichte, T. Kratzke, S. Kaskel, *Microporous Mesoporous Mater.* 2004, 73, 81–88; k) T. Arai, H. Takasugi, T. Sato, H. Noguchi, H. Kanoh, K. Kaneko, A. Yanagisawa, *Chem. Lett.* 2005, 34, 1590–1591; l) S. Ishida, T. Hayano, H. Furuno, J. Inanaga, *Heterocycles* 2005, 66, 645–649; m) W. Chen, R. Li, Y. Wu, L. S. Ding, Y. C. Chen, *Synthesis* 2006, 3058–3062; n) Y. M. A. Yamada, Y. Maeda, Y. Uozumi, *Org. Lett.* 2006, 8, 4259–4262; o) H. Han, S. Zhang, H. Hou, Y. Fan, Y. Zhu, *Eur. J. Inorg. Chem.* 2006, 1594–1600; p) K. H. Park, K. Jang, S. U. Son, D. A. Sweigart, *J. Am. Chem. Soc.* 2006, 128, 8740–8741; q) L. Alaerts, E. Seguin, H. Poelman, F. Thibault-Starzyk, P. A. Jacobs, D. E. De Vos, *Chem. Eur. J.* 2006, 12, 7353–7363; r) U. Mueller, M. Schubert, F. Teich, H. Puetter, K. Schierle-Arndt, J. Pastre, *J. Mater. Chem.* 2006, 16, 626–636; s) P. Horcajada, S. Surble, C. Serre, D. Y. Hong, Y. K. Seo, J. S. Chang, J. M. Greneche, I. Margiolaki, G. Férey, *Chem. Commun.* 2007, 2820–2822; t) F. X. L. I. Xamena, A. Abad, A. Corma, H. Garcia, *J. Catal.* 2007, 250, 294–298; u) S. Hasegawa, S. Horike, R. Matsuda, S. Furukawa, K. Mochizuki, Y. Ki-

- noshita, S. Kitagawa, *J. Am. Chem. Soc.* **2007**, *129*, 2607–2614; v) S. Horike, M. Dinka, K. Tamaki, J. R. Long, *J. Am. Chem. Soc.* **2008**, *130*, 5854–5855; w) U. Ravon, M. E. Domine, C. Gaudillère, A. Desmartin-Chomel, D. Farrusseng, *New J. Chem.* **2008**, *32*, 937–940; x) D. Jiang, T. Mallat, F. Krumeich, A. Baiker, *J. Catal.* **2008**, *257*, 390–395; y) A. Henschel, K. Gedrich, R. Kraehnert, S. Kaskel, *Chem. Commun.* **2008**, 4192–4194.
- [10] J. S. Seo, D. Whang, H. Lee, S. I. Jun, J. Oh, Y. J. Jeon, K. Kim, *Nature* **2000**, *404*, 982–986.
- [11] a) S. Takizawa, H. Somei, D. Jayaprakash, H. Sasai, *Angew. Chem.* **2003**, *115*, 5889–5892; *Angew. Chem. Int. Ed.* **2003**, *42*, 5711–5714; b) H. Guo, X. Wang, K. Ding, *Tetrahedron Lett.* **2004**, *45*, 2009–2012; c) X. Wang, X. Wang, H. Guo, Z. Wang, K. Ding, *Chem. Eur. J.* **2005**, *11*, 4078–4088.
- [12] a) H. L. Ngo, A. G. Hu, W. Lin, *J. Mol. Catal. A* **2004**, *215*, 177–186; b) C.-D. W. A. Hu, L. Zhang, W. Lin, *J. Am. Chem. Soc.* **2005**, *127*, 8940–8941; c) C. D. Wu, W. Lin, *Angew. Chem.* **2007**, *119*, 1093–1096; *Angew. Chem. Int. Ed.* **2007**, *46*, 1075–1078.
- [13] a) X. Wang, L. Shi, M. Li, K. Ding, *Angew. Chem.* **2005**, *117*, 6520–6524; *Angew. Chem. Int. Ed.* **2005**, *44*, 6362–6366; b) S. H. Cho, B. Ma, S. T. Nguyen, J. T. Hupp, T. E. brecht-Schmitt, *Chem. Commun.* **2006**, 2563–2565; c) S. H. Cho, T. Gadzikwa, M. Afshari, S. T. Nguyen, J. T. Hupp, *Eur. J. Inorg. Chem.* **2007**, 4863–4867.
- [14] J. I. García, B. López-Sánchez, J. A. Mayoral, *Org. Lett.* **2008**, *10*, 4995–4998.
- [15] K. Tanaka, S. Oda, M. Shiro, *Chem. Commun.* **2008**, 820–822.
- [16] a) A. Hu, H. L. Ngo, W. Lin, *J. Am. Chem. Soc.* **2003**, *125*, 11490–11491; b) A. Hu, H. L. Ngo, W. Lin, *Angew. Chem.* **2003**, *115*, 6182–6185; *Angew. Chem. Int. Ed.* **2003**, *42*, 6000–6003; c) X. Wang, K. Ding, *J. Am. Chem. Soc.* **2004**, *126*, 10524–10525; d) Y. Liang, Q. Jing, X. Li, L. Shi, K. Ding, *J. Am. Chem. Soc.* **2005**, *127*, 7694–7695; e) L. Shi, X. Wang, C. A. Sandoval, M. Li, Q. Qi, Z. Li, K. Ding, *Angew. Chem.* **2006**, *118*, 4214–4218; *Angew. Chem. Int. Ed.* **2006**, *45*, 4108–4112.
- [17] For leading references of AH by using monodentate phosphorous ligands, see: a) M. van den Berg, A. J. Minnaard, E. P. Schudde, J. van Esch, A. H. M. de Vries, J. G. de Vries, B. L. Feringa, *J. Am. Chem. Soc.* **2000**, *122*, 11539–11540; b) M. T. Reetz, G. Mehler, *Angew. Chem.* **2000**, *112*, 4047–4049; *Angew. Chem. Int. Ed.* **2000**, *39*, 3889–3890; c) C. Claver, E. Fernandez, A. Gillon, K. Heslop, D. J. Hyett, A. Martorell, A. G. Orpen, P. G. Pringle, *Chem. Commun.* **2000**, 961–962; d) I. V. Komarov, A. Börner, *Angew. Chem.* **2001**, *113*, 1237–1240; *Angew. Chem. Int. Ed.* **2001**, *40*, 1197–1200; e) A.-G. Hu, Y. Fu, J.-H. Xie, H. Zhou, L.-X. Wang, Q.-L. Zhou, *Angew. Chem.* **2002**, *114*, 2454–2456; *Angew. Chem. Int. Ed.* **2002**, *41*, 2348–2350; f) S. Wu, W. Zhang, Z. Zhang, X. Zhang, *Org. Lett.* **2004**, *6*, 3565–3567; g) Y. Liu, K. Ding, *J. Am. Chem. Soc.* **2005**, *127*, 10488–10489.
- [18] This has been borne out in some case studies using monodentate phosphorus ligands for Rh<sup>I</sup>-catalyzed hydrogenation reactions. See, for example: a) M. T. Reetz, A. Meiswinkel, G. Mehler, K. Angermund, M. Graf, W. Thiel, R. Mynott, D. G. Blackmond, *J. Am. Chem. Soc.* **2005**, *127*, 10305–10313; b) I. D. Gridnev, C. Fan, P. G. Pringle, *Chem. Commun.* **2007**, 1319–1321, and references therein. See also ref. [17g].
- [19] The coordinating ligand has been included as part of the polymer mass used. Possible enclathration of the solvent in the polymer was not considered in the calculation for simplicity.
- [20] M. van den Berg, A. J. Minnaard, R. M. Haak, M. Leeman, E. P. Schudde, A. Meetsma, B. L. Feringa, A. H. M. de Vries, C. E. P. Maljaars, C. E. Willans, D. Hyett, J. A. F. Boogers, H. J. W. Henderickx, J. G. de Vries, *Adv. Synth. Catal.* **2003**, *345*, 308–323.
- [21] Turnover number (TON) is defined as moles of product per mole of catalyst, and turnover frequency (TOF) is defined as TON per hour or second.
- [22] The reaction profiles for **4c,d,f** under analogous conditions are given in the Supporting Information, Figure S4.
- [23] However, the same homogeneous catalyst is faster (TOF = 190 h<sup>-1</sup> at 2 atm) when CH<sub>2</sub>Cl<sub>2</sub> is used as solvent, whereas the *ee* for **6b** is 96% (Supporting Information, Figure S4).
- [24] a) B. Pugin, *J. Mol. Catal. A* **1996**, *107*, 273–279; b) K. Mashima, T. Hino, H. Takaya, *Tetrahedron Lett.* **1991**, *32*, 3101–3104.
- [25] a) J. M. Brown, P. A. Chaloner, *J. Chem. Soc. Chem. Commun.* **1978**, 321; b) J. Halpern, A. S. C. Chan, J. J. Pluth, *J. Am. Chem. Soc.* **1980**, *102*, 5952–5954; c) I. D. Gridnev, T. Imamoto, *Acc. Chem. Res.* **2004**, *37*, 633–644; T. Schmidt, W. Baumann, H.-J. Drexler, A. Arrieta, D. Heller, H. Buschmann, *Organometallics* **2005**, *24*, 3842–3848; d) H.-J. Drexler, W. Baumann, T. Schmidt, S. Zhang, A. Sun, A. Spannenberg, C. Fischer, H. Buschmann, D. Heller, *Angew. Chem.* **2005**, *117*, 1208–1212; *Angew. Chem. Int. Ed.* **2005**, *44*, 1184–1188.
- [26] a) S. Saaby, K. R. Knudsen, M. Laddow, S. C. Ley, *Chem. Commun.* **2005**, 2909–2911; b) N. Yoswathananont, K. Nitta, Y. Nishiuchi, M. Sato, *Chem. Commun.* **2005**, 40–42; c) J. Kobayashi, Y. Mori, K. Okamoto, R. Akiyama, M. Ueno, T. Kitamori, S. Kobayashi, *Science* **2004**, *304*, 1305–1308; d) J. Kobayashi, Y. Mori, S. Kobayashi, *Adv. Synth. Catal.* **2005**, *347*, 1889–1892.
- [27] Other hydride sources: a) A. J. Sandee, D. G. I. Petra, J. N. H. Reek, P. C. J. Kamer, P. W. N. M. van Leewen, *Chem. Eur. J.* **2001**, *7*, 1202–1208; b) W. Solodenko, H. Wen, S. Leue, F. Stuhlmann, G. Sourkouni-Argirusi, G. Jas, H. Schönfeld, U. Kunz, A. Kirschning, *Eur. J. Org. Chem.* **2004**, 3601–3610.
- [28] For selected reviews on continuous flow reactors and processes, see: a) A. Kirschning, W. Solodenko, K. Mennecke, *Chem. Eur. J.* **2006**, *12*, 5972–5990; b) C. Wiles, P. Watts, *Eur. J. Org. Chem.* **2008**, 1655–1671. For recent examples, see: c) Y. Uozumi, Y. M. A. Yamada, T. Beppu, N. Fukuyama, M. Ueno, T. Kitamori, *J. Am. Chem. Soc.* **2006**, *128*, 15994–15995; d) C. D. Smith, I. R. Baxendale, S. Lanners, J. J. Hayward, S. C. Smith, S. V. Ley, *Org. Biomol. Chem.* **2007**, *5*, 1559–1561.

Received: April 5, 2009  
Published online: August 15, 2009